Catalysis Science & Technology

Production of Novel Rieske Dioxygenase Metabolites Enabled by Enzyme Engineering

Journal:	*Catalysis Science & Technology*
Manuscript ID	CY-COM-02-2023-000262.R1
Article Type:	Communication
Date Submitted by the Author:	22-May-2023
Complete List of Authors:	Osifalujo, Elizabeth; Ball State University, Chemistry Rutkowski, Bailey; Ball State University, Chemistry Satterwhite, Louis; Ball State University, Chemistry Betts, Phillip; Ball State University, Chemistry Nkosi, Angel; Ball State University, Chemistry Froese, Jordan; Ball State University, Chemistry

COMMUNICATION

Production of Novel Rieske Dioxygenase Metabolites Enabled by Enzyme Engineering

Received 00th January 20xx,
Accepted 00th January 20xx

DOI: 10.1039/x0xx00000x

Elizabeth A. Osifalujo,[a] Bailey N. Rutkowski,[a] Louis R. Satterwhite,[a] Phillip C. Betts,[a] Angel K. Nkosi,[a] and Jordan T. Froese*[a]

Despite their popularity as enantioselective catalysts, the range of applications for Rieske dioxygenases has remained limited by their substrate scopes and selectivity. Herein, we report the development of dioxygenase variants with expanded substrate scopes through rational enzyme engineering. These catalysts have enabled the production of novel and valuable chiral metabolites.

The enantioselective dihydroxylation of aromatics is an important process that has found utility in the production of a wide variety of valuable compounds (**Figure 1**).[1] These dearomatization processes have frequently been achieved using Rieske dioxygenases (RDOs),[1] a class of enzymes commonly found in soil bacteria.[2] In their native context, RDOs, which consist of reductase, ferredoxin, and oxidase components, play an important role in the metabolic pathways by which soil organisms break down aromatic pollutants in their environment.[2] In addition to their ability to catalyze the enantioselective dihydroxylation of aromatics, RDOs have also demonstrated the capability to effect sulfoxidation, C-H amination, desaturation, and monohydroxylation.[3-6] Owing to this tremendous versatility, as well as the growing recognition of the value of environmentally sustainable catalytic methods, RDO enzymes have remained a popular tool in the field of organic synthesis.[1]

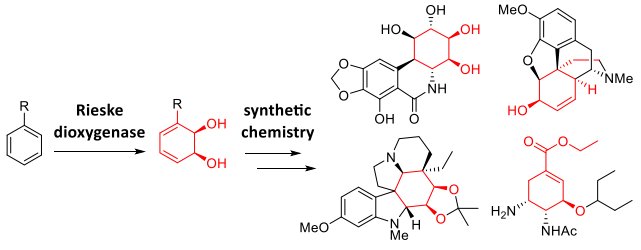

Figure 1: Enantioselective oxidative dearomatization catalyzed by Rieske dioxygenases, and examples of the synthetic application of the resultant metabolites.[1f,l,n,o,x]

Despite the catalytic versatility demonstrated by RDOs, the substrate scope and activity of these enzymes remain limited by the steric and electrostatic demands of potential substrates.[7-9] As a result of these restrictions on the activity and selectivity of the native enzymes, the range of synthetic applications for RDOs has remained limited. To alleviate these constraints on the range of applications for RDOs, enzyme engineering has been applied to expand their substrate scopes and to improve the activity of these enzymes for specific classes of substrates.[9] These studies have been successful both in improving the activity of RDOs for specific substrate classes, making their application in organic synthesis more practical,[9d,e,m,t,x,10] and in developing RDO variants with activity for entirely new substrates.[9,h,n,o,q]

Owing to the fact that many RDOs have evolved to metabolize non-polar aromatics,[2,11] and their active sites are therefore organized to bind non-polar substrates,[12] engineering RDO variants that can effectively bind and metabolize more polar substrates remains a challenge. Recently, our laboratory reported engineering studies that applied active site-targeted rational mutagenesis and high-throughput screening to produce toluene dioxygenase (TDO) variants with significantly improved activity for ester-functionalized aromatics.[10] Because the native TDO enzyme can metabolize these ester-functionalized substrates at only a very low level,[1g,j,r,7] the availability of these engineered variants has made the application of the corresponding chiral metabolites in organic synthesis much more practical. The success of this study led our group to expand these engineering efforts, as we aim to develop new TDO variants that can metabolize substrates for which the native enzyme has no discernible activity. The success of such efforts would provide access to new and potentially valuable chiral synthons to the synthetic community and would expand the range of

[a] *Department of Chemistry, Ball State University, 1600 W Ashland Ave, Muncie, IN, 47303, USA.*

Electronic Supplementary Information (ESI) available: [details of any supplementary information available should be included here]. See DOI: 10.1039/x0xx00000x

applications for these environmentally benign enzymatic catalysts.

Prior to this study, no native or engineered RDO has been available that can perform the 2,3-dihydroxylation of amine or amide functionalized aromatics. This has left a gap in the range of *cis*-diol metabolites available for use as chiral synthons in organic synthesis. As a result, synthetic efforts targeting high-value compounds that contain these functional groups have required circuitous routes to introduce these functional groups into other *cis*-diol metabolites (**Figure 2**).[1t] In an effort to expand upon the range of synthetic applications available for RDOs, and based upon previous success developing RDO variants with improved activity for polar substrates,[10] our laboratory determined to attempt the engineering of TDO variants with activity for amide-functionalized substrates.

Based upon the success of our previous study, which employed a rational engineering approach, eight active site residues were selected for saturation mutagenesis (M220, A223, L272, I276, V309, L321, I324, and F366, **Figure 3**), based on their proximity to the (native) substrate when it is bound to the active site (M220 – 4.9 Å, A223 – 3.9 Å, L272 – 5.1 Å, I276 – 5.2 Å, V309 – 4.5 Å, L321 – 3.8 Å, I324 – 4.9 Å, F366 – 4.3 Å, **Figure 3**)[12b] and based on previous results from our lab and others.[9x,10] Individual saturation mutagenesis libraries were generated by mutating each of the described positions using established methods.[15] A previously reported modern expression platform for the TDO enzyme system was used as the template for mutagenesis.[13] The individual mutant plasmid libraries were then transformed into *E. coli* (BL21 (DE3)), and single colonies were cultured in 96-well plates according to our reported, optimized protocols.[10] 176 members of each variant library were cultured and the biotransformation reactions were carried out in 96-well plates using the model substrate for this study, *N*-benzylacetamide. Using a recently reported high-throughput, fluorescence-based assay system (**Figure 4A**),[13] the *cis*-dihydroxylation activity of each variant library member for the model substrate was assessed alongside the parent enzyme and the negative controls (pCP-01).[13] Among the eight enzyme variant libraries screened in this way, three (L272, I276, V309) contained library members that demonstrated significant activity for the model substrate (*N*-benzylacetamide). Representative screening data for the TDO L272 variant library is shown in **Figure 4B**. To confirm the described activity observed from the primary screens, plasmid DNA from all putative hits was isolated and retransformed into *E. coli* (BL21

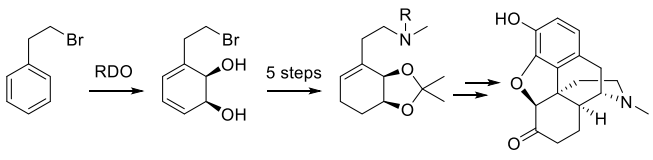

Figure 2: Application of the *cis*-diol metabolite produced from (2-bromoethyl) benzene in the synthesis of *ent*-hydromorphone.[1t]

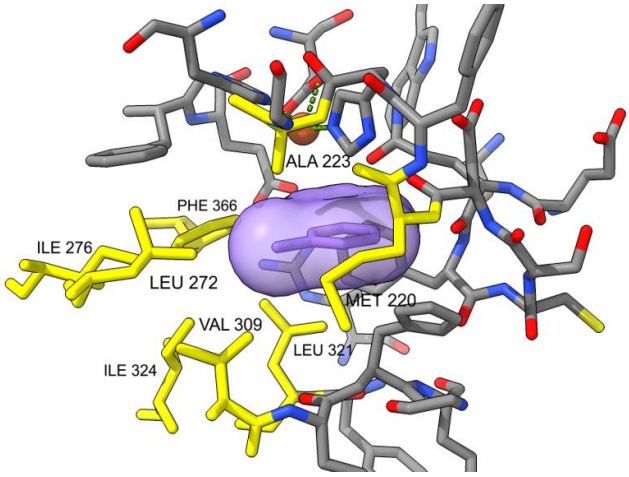

Figure 3: Visualization of the TDO active site with the native substrate bound (toluene, purple).[12b] Residues within 7 Å of the substrate are shown. Residues selected for saturation mutagenesis are highlighted (yellow). Image generated with ChimeraX software.[14]

(DE3)). Cultures expressing variants identified as putative hits were then carried through the biotransformation and assay protocol a second time, validating the results from primary screens. All variants with confirmed activity upon secondary screening were then sequenced to identify any beneficial mutations. This sequencing analysis revealed five distinct point mutations that conferred activity for the amide-functionalized substrate (L272F, L272W, I276V, V309G, and V309N). Among these point mutations, I276V and V309G had previously been shown by our group to confer improved activity for ester-functionalized substrates,[10] with V309G also having been shown to improve TDO activity for sterically bulky substrates in other studies.[9x]

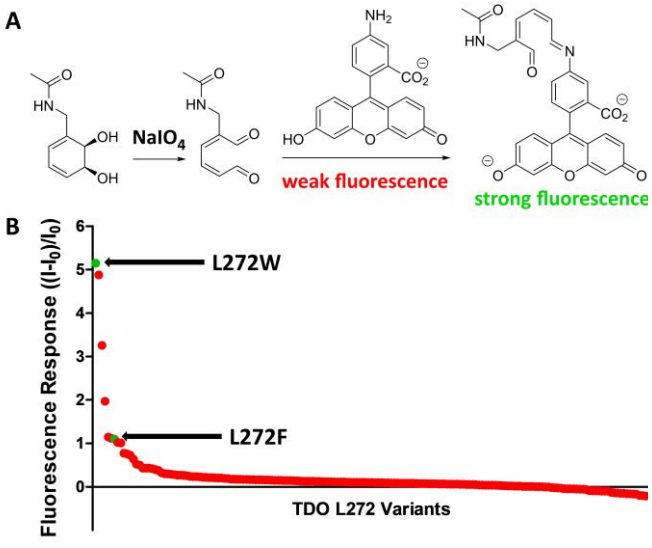

Figure 4: (A) Coupled reactions employed by the fluorescence-based assay to detect and quantify the *cis*-diol metabolites produced by active RDOs;[13] (B) Activity of the TDO L272 variant library members for the *N*-benzylacetamide substrate (n = 176). Fluorescence response of each variant was normalized to the mean fluorescence response of the negative controls (*E. coli* BL21 (DE3) pCP-01)[13] ($([I - I_0]/I_0)$ (n = 4).

To accurately assess the relative activity of these improved TDO variants, their *cis*-dihydroxylation activity for both the model substrate (*N*-benzylacetamide) and the more sterically demanding substrate *N*-(2-phenethyl)acetamide were tested in parallel (**Figure 5A**). The results of these assays clearly demonstrated that the TDO L272W variant possessed the highest activity for *N*-benzylacetamide, while TDO V309G possessed the highest activity for *N*-(2-phenethyl)acetamide (**Figure 5A**). Only the TDO L272W and TDO V309G variants demonstrated any activity for the *N*-(2-phenethyl)acetamide substrate. The activity of these variants for the native substrate (toluene) and the related non-polar substrate ethylbenzene were also tested, revealing that, with the exception of the V309N variant, each variant retained approximately equal levels of activity for the native substrate (**Figure S5**). The V309G mutant demonstrated ~30% improvement in activity for the ethylbenzene substrate, while the V309N variant lacked any activity for the native substrate and demonstrated a significant decrease in activity for ethylbenzene (**Figure S5**).

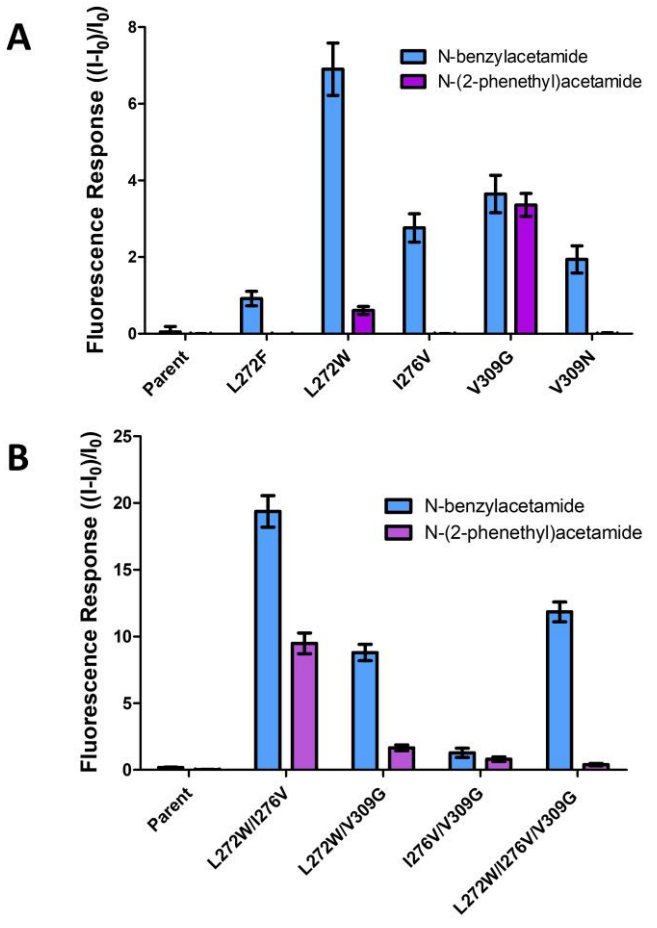

Figure 5: (A) Relative activity of variants bearing single active site mutations for *N*-benzylacetamide and *N*-(2-phenethyl)acetamide substrates compared to the parent enzyme (n = 6). Fluorescence response of each variant was normalized to the mean fluorescence response of the negative controls (*E. coli* BL21 (DE3) pCP-01)[13] ($[I - I_0]/I_0$) (n = 6). (B) Relative activity of doubly and triply combined variants for *N*-benzylacetamide and *N*-(2-phenethyl)acetamide substrates compared to the parent enzyme (n = 6). Fluorescence response of each variant was normalized to the mean fluorescence response of the negative controls (*E. coli* BL21 (DE3) pCP-01)[13] ($[I - I_0]/I_0$) (n = 6).

As previous studies in our laboratory and in others have shown that combining beneficial substitutions can result in further increases in enzyme variant activity,[9x,10] it was determined to generate doubly and triply combined mutants based on the individual point mutations that had been identified as beneficial for activity on amide-functionalized substrates. By utilizing the vector systems containing the most beneficial single active site mutations as templates (L272W, I276V, V309G), three doubly combined variants were generated (L272W/I276V, L272W/V309G, I276V/V309G), along with one triply combined variant (L272W/I276V/V309G), using established methods.[15] The activity of these combined variants for both the *N*-benzylacetamide and *N*-(2-phenethyl)acetamide substrates were then tested in parallel (**Figure 5B**). Based on the results of these assays, the doubly combined TDO L272W/I276V variant clearly demonstrated the highest activity for both *N*-benzylacetamide and *N*-(2-phenethyl)acetamide of any variant evaluated in this study (**Figure 5B**). The L272W/I276V and I276V/V309G variants demonstrated approximately parental levels of activity for both the native substrate (toluene) and ethylbenzene, while the introduction of the L272W/V309G and the L272W/I276V/V309G mutations resulted in significant decreases in activity for the native substrate (**Figure S5**).

With the *cis*-diol metabolites produced from the enzymatic dihydroxylation of both *N*-benzylacetamide and *N*-(2-phenethyl)acetamide being previously unknown compounds (**1** and **2**, **Figure 6**), medium-scale (1 L) biotransformations were performed with both substrates using TDO L272W/I276V as the catalyst, to produce sufficient quantities of the metabolites for isolation and characterization. Spectroscopic and spectrometric analysis of both compounds confirmed their identity as predicted, with the regioselectivity of the enzymatic dihydroxylation of both substrates being confirmed through correlation spectroscopy (COSY-NMR) (**Figures S7 and S9**) and through comparison to previously characterized *cis*-diol metabolites (**Figure S10**). This proposed regioselectivity of the enzymatic dihydroxylation is also supported by docking studies discussed below.

Given the fact that the TDO I276V variant has previously been shown by our lab to confer improved activity for ester-functionalized substrates,[10] and that the TDO V309G variant has similarly been shown to confer improved activity for both ester-functionalized and sterically bulky substrates,[9x,10] the

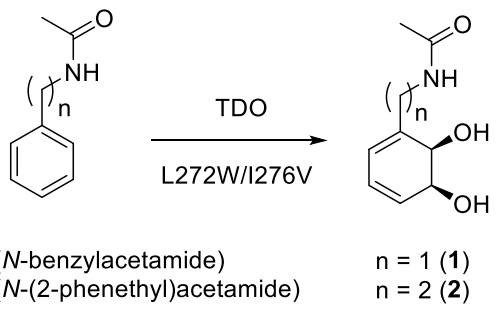

Figure 6: Production of novel chiral metabolites (**1** and **2**) from *N*-benzylacetamide and *N*-(2-phenethyl)acetamide using the engineered TDO L272W/I276V variant as the catalyst.

identification of these variants in this study was not unexpected. Based on previous reports, it is likely that the improved/novel activity that these mutations afford is the result of increased space in the active site,[9x,10] which may explain the ability of these variants to bind and metabolize *N*-benzylacetamide and/or *N*-(2-phenethyl)acetamide, which are sterically larger than the native substrate (toluene). The remaining three beneficial substitutions identified in this study (L272F, L272W, and V309N) however, have not previously been identified as beneficial in any study, and the mechanism by which they afford novel activity is less intuitive. To investigate these mechanisms, homology modeling was performed using Alphafold2[16] to generate structures of these three variants. Using these homology models, the active site cavity was mapped for each variant using PyMOL.[17] Based upon this analysis, the L272F mutation does not appear to significantly affect the size of the active site cavity (**Figure S11**). However, docking analysis performed with Autodock Vina[18] did predict an improvement in affinity for the *N*-benzylacetamide substrate with the TDO L272F homology model compared to the affinity observed when docking this substrate with the native enzyme (**Table 1**). These docking predictions were further analyzed through molecular dynamics simulations performed with GROMACS,[19] which also revealed improved nonbonded interaction energy between the L272F homology model and *N*-benzylacetamide over the wild-type enzyme (**Table 1**). Unlike the L272F mutation, the V309N mutation does appear to slightly increase the size of the TDO active site cavity (**Figure S13**). Docking studies between the TDO V309N homology model and *N*-benzylacetamide yielded an identical affinity to that observed with the TDO L272F homology model, with molecular dynamics simulation revealing slightly improved nonbonded interaction energy for TDO V309N over TDO L272F (**Table 1**). This may be due to favorable interactions between the polar amide substituent of the substrate and the polar side chain of asparagine, with the docking results positioning these groups ~3.2 Å apart (**Figure S14**).

Table 1: Binding affinities and nonbonded interaction energies for *N*-benzylacetamide and *N*-(2-phenethyl)acetamide among selected TDO variants and the wild-type TDO enzyme, as predicted by AutoDock Vina[18] and GROMACS[19] respectively. All docking studies and molecular dynamics simulations utilized homology models generated by Alphafold2,[16] with the exception of wild-type enzyme docking which utilized the reported crystal structure of this enzyme.[12b]

	Ligand			
	N-benzylacetamide		*N*-(2-phenethyl)acetamide	
Enzyme	Affinity (kcal/mol)	Nonbonded interaction energy* (kcal/mol)	Affinity (kcal/mol)	Nonbonded interaction energy* (kcal/mol)
TDO (WT)	-5.9	-24.7 (1.0)	-6.4	-24.4 (0.5)
TDO L272F	-6.7	-32.3 (0.6)	-7.1	-24.9 (0.4)
TDO V309N	-6.7	-33.9 (0.3)	-6.8	-33.7 (1.1)
TDO L272W	-6.6	-30.8 (0.6)	-6.8	-29.7 (0.9)
TDO L272W/I276V	-6.8	-29.3 (0.7)	-6.5	-25.3 (0.5)

*Calculated from the combined average short-range Coulombic interaction energy and the short-range Lennard-Jones energy, as predicted by GROMACS.[19]

The most unexpected of the beneficial point mutations identified in this study was the TDO L272W mutation. This mutation conferred by far the greatest activity for the *N*-benzylacetamide substrate of any single mutation, however, it was expected that this mutation would significantly reduce the size of the active site cavity. Mapping of the active site cavity in the TDO L272W variant, using a homology model generated with Alphafold2,[16] refuted the hypothesis that substituting an active site leucine for tryptophan would significantly decrease the space in the active site (**Figure 7**). Although it is theoretically possible to envision a stabilizing interaction between the amide substituent of the substrate and the indole ring of the tryptophan residue, docking studies combined with molecular dynamics simulations do not predict such an interaction owing to the predicted positioning of the indole ring in the active site of the TDO L272W homology model (**Figure 7C**). Docking studies did predict an increase in binding affinity between TDO L272W and *N*-benzylacetamide relative to the wild-type enzyme, and molecular dynamics simulations indicated improved nonbonded interaction energy for TDO L272W with *N*-benzylacetamide over the wild-type enzyme (**Table 1**). However, despite demonstrating the highest activity for *N*-benzylacetamide among the TDO variants with single

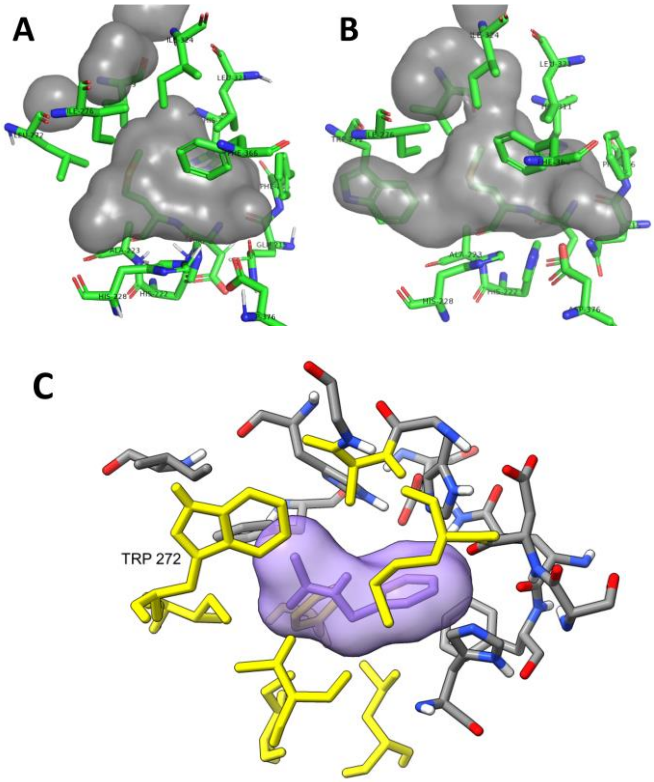

Figure 7: (A) Visualization of the active site cavity of TDO (wild-type). Image generated using the reported crystal structure of TDO[12b] and with PyMOL.[17] (B) Visualization of the active site cavity of TDO L272W. Image generated using a homology model of TDO L272W and with PyMOL.[17] (C) Active site structure produced from molecular dynamics simulations performed on the docking prediction of TDO L272W with *N*-benzylacetamide (purple). The relative positioning of the W272 residue is shown. Residues targeted for mutagenesis in this study are highlighted (yellow). Docking was performed with AutoDock Vina,[19] using a TDO L272W homology model. Molecular dynamics simulations were performed with GROMACS.[19] Image was generated using ChimeraX software.[14]

mutations identified in this study, the TDO L272W homology model was predicted to have slightly reduced affinity and nonbonding interaction energy with this substrate relative to the L272F and V309N variants (**Table 1**). Further studies are ongoing to more clearly elucidate the source of the increase in activity observed for *N*-benzylacetamide with the TDO L272W variant and will be reported in due course.

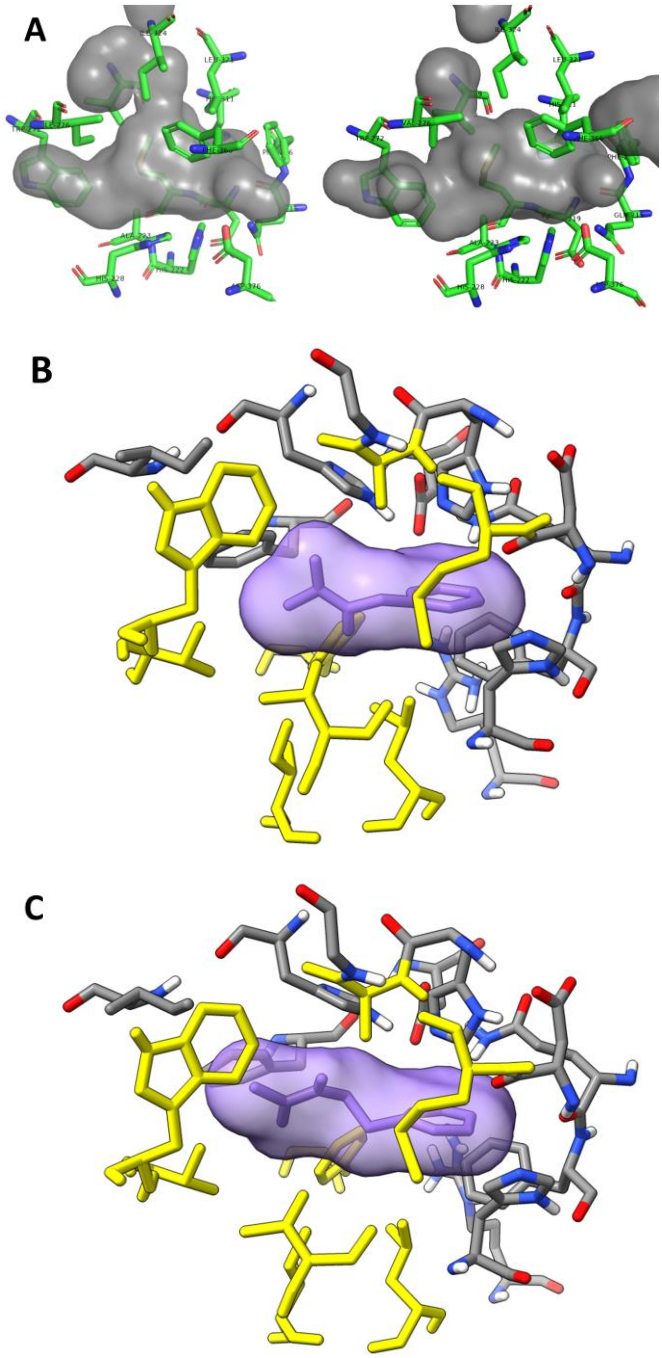

Figure 8: (A) Comparison of the active site cavities of TDOL272W (left) and TDO L272W/I276V (right). Images were generated using homology models of TDO L272W and TDO L272W/I276V with bound substrate and with PyMOL.[17] (B) Active site structure produced from molecular dynamics simulations performed on the docking prediction of TDO L272W/I276V with *N*-benzylacetamide (purple). Residues targeted for mutagenesis in this study are highlighted (yellow). Docking was performed with AutoDock Vina,[19] using a TDO L272W/I276V homology model. Molecular dynamics simulations were performed with GROMACS.[19] Image was generated using ChimeraX software.[14] (C) Active site structure produced from molecular dynamics simulations performed on the docking prediction of TDO L272W/I276V with *N*-(2-phenethyl)acetamide (purple). Residues targeted for mutagenesis in this study are highlighted (yellow). Docking was performed with AutoDock Vina,[19] using a TDO L272W/I276V homology model. Molecular dynamics simulations were performed with GROMACS.[19]Image was generated using ChimeraX software.[14]

Given that the TDO L272W/I276V variant demonstrated the highest activity for both the *N*-benzylacetamide and *N*-(2-phenethyl)acetamide substrates among all the variants evaluated in this study, a homology model of this variant was also generated using Alphafold2[16] to investigate the active site structure and substrate binding. The introduction of this mutation appears to further remodel the active site, resulting in slightly increased space relative to the TDO L272W variant (**Figure 8A**). This is reflected in the improved binding affinity between TDO L272W/I276V and *N*-benzylacetamide relative to all other enzymes assessed in this way (**Table 1**). However, although the TDO L272W/I276V variant showed significantly improved nonbonded interaction energy with *N*-benzylacetamide from molecular dynamics simulations relative to the wild-type enzyme, this variant had slightly reduced nonbonded interaction energy with *N*-benzylacetamide relative to the TDO L272W, V309N, and L272F variants, which demonstrated lower activity for this substrate (**Table 1**). Again, although it is possible to envision a stabilizing interaction between the amide substituent of the substrate and the indole ring of the tryptophan residue, docking studies combined with molecular dynamics simulations do not predict such an interaction owing to the positioning of the indole ring in the active site of the TDO L272W/I276V homology model (**Figure 8B**). Interestingly, although the TDO L272W/I276V variant demonstrated by far the greatest activity for the *N*-(2-phenethyl)acetamide substrate among all of the variants assessed in this study, docking studies predicted that this variant would have a lower binding affinity for *N*-(2-phenethyl)acetamide than the TDO L272F, V309N, and L272W variants, with only slightly improved binding affinity over the wild type enzyme, which does not possess any activity for this substrate (**Table 1**). A similar trend was observed in analyzing the nonbonded interaction energies between these enzymes and *N*-(2-phenethyl)acetamide through molecular dynamics simulations (**Table 1**). Further studies are ongoing to more clearly elucidate the source of the increase in activity observed for *N*-benzylacetamide and *N*-(2-phenethyl)acetamide with the TDO L272W/I276V variant and will be reported in due course.

Conclusions

In this study, new variants of toluene dioxygenase (TDO) were rationally engineered that possess activity for amide-functionalized substrates, which cannot be metabolized by the wild-type enzyme. These engineered TDO variants afforded access to multiple new chiral metabolites which were isolated and characterized. In this way, this study has added to the pool of chiral synthons available for application in organic synthesis and provided new and valuable green-chemical tools to the chemical community. To account for the novel activity observed with these engineered TDO variants, homology

modeling, docking analyses, and molecular dynamics simulations were performed using Alphafold2,[16] AutoDock Vina,[18] and GROMACS[19] respectively. Although these studies cannot fully account for the level of activity observed among the engineered TDO variants, as the computed binding affinities and nonbonded interaction energies do not directly correlate with their observed activity levels, they do provide important indications as to the potential source(s) of this novel activity. These sources may include increases in the size of the TDO binding pocket facilitating the binding of amide-functionalized substrates which are sterically larger than the native substrate, and the potential introduction of new non-covalent bonding partners for the bound substrates.

Acknowledgements

This material is based upon work supported by the National Science Foundation under Grant No. 2147098 (Research in Undergraduate Institutions) and by the Ball State University Junior Faculty ASPiRE grant program. This work was made possible in part by the Ball State University Provost Start-Up program.

Conflicts of interest

There are no conflicts to declare.

Notes and references

1 Selected examples of the application of Rieske dioxygenase metabolites in synthesis: (a) A. M. Reiner, *J. Bacteriol*., 1971, **108**, 89; (b) W.-K. Yeh, D. T. Gibson and T.-N. Liu, *Biochem. Biophys. Res. Commun*., 1977, **78**, 401; (c) V. Subramanian, T.-N. Liu, W. K. Yeh and D. T. Gibson, *Biochem. Biophys. Res. Commun*., 1979, **91**, 1131; (d) D. A. Widdowson, D. W. Ribbons and S. D. Thomas, *Janssen Chim. Acta,* 1990, **8**, 3; (e) T. Hudlicky and J. W. Reed, in *Advances in Asymmetric Synthesis* (Ed. A. Hassner), JAI Press, Greenwich, 1995, pp. 271; (f) X. Tian, T. Hudlicky and K. Königsberger, *J. Am. Chem. Soc*., 1995, **117**, 3643; (g) T. Hudlicky and A. J. Thorpe, *Chem. Commun*., 1996, 1993; (h) T. Hudlicky, D. A. Entwistle, K. K. Pitzer and A. J. Thorpe, *Chem. Rev*., 1996, **96**, 1195; (i) D. R. Boyd and G. N. Sheldrake, *Nat. Prod. Rep*., 1998, **15**, 309; (j) M. A. Endoma, V. P. Bui, J. Hansen and T. Hudlicky, *Org. Process Res. Dev*., 2002, **6**, 525; (k) M. G. Banwell, A. J. Edwards, G. J. Harfoot, K. A. Jolliffe, M. D. McLeod, K. J. McRae, S. G. Stewart and M. Vogtle, *Pure Appl. Chem*., 2003, **75**, 223; (l) A. T. Omori, K. J. Finn, H. Leisch, R. J. Carroll and T. Hudlicky, *Synlett,* 2007, 2859; (m) T. Hudlicky and J. W. Reed, *Synlett,* 2009, 685; (n) B. Sullivan, I. Carrera, M. Drouin and T. Hudlicky, *Angew. Chem., Int. Ed*., 2009, **48**, 4229; (o) L. Werner, A. Machara and T. Hudlicky, *Adv. Synth. Catal*., 2010, **352**, 195; (p) J. F. Trant, J. Froese and T. Hudlicky, *Tetrahedron-Asymmetry*, 2013, **24**, 184; (q) D. K. Winter, M. A. Endoma-Arias, T. Hudlicky, J. A. Beutler and J. A. Porco, Jr. *J. Org. Chem*., 2013, **78**, 7617; (r) M. A. A. Endoma-Arias, J. R. Hudlicky, R. Simionescu and T. Hudlicky, *Adv. Synth. Catal*., 2014, **356**, 333; (s) S. E. Lewis, *Chem. Commun*., 2014, **50**, 2821; (t) V. Varghese and T. Hudlicky, *Angew. Chem., Int. Ed*., 2014, **53**, 4355; (u) S. Vshyvenko, M. R. Reisenauer, S. Rogelj and T. Hudlicky, *Bioorg. Med. Chem. Lett*., 2014, **24**, 4236; (v) S. E. Lewis, in *Asymmetric Dearomatization Under Enzymatic Conditions* (Ed. S.-L. You), Wiley, Chichester, 2016, p. 279; (w) J. Froese, C. Overbeeke and T. Hudlicky, *Chem. – Eur. J*., 2016, **22**, 6180; (x) L. V. White, M. G. Banwell, *J. Org. Chem*. **2016**, *81*, 1617–1626; (y) D. Baidilov, L. Rycek, J. F. Trant, J. Froese, B. Murphy and T. Hudlicky, *Angew. Chem., Int. Ed*., 2018, **57**, 10994; (z) D. R. Boyd, N. D. Sharma, P. L. Loke, J. G. Carroll, P. J. Stevenson, P. Hoering and C. C. R. Allen, *Front. Bioeng. Biotechnol*., 2021, **8**, 619175.

2 (a) D. T. Gibson, J. R. Koch and R. E. Kallio, *Biochemistry,* 1968, **7**, 2653; (b) D. T. Gibson, J. R. Koch, C. L. Schuld and R. E. Kallio, *Biochemistry,* 1968, **7**, 3795; (c) D. T. Gibson, M. Hensley, H. Yoshioka and T. J. Mabry, *Biochemistry,* 1970, **9**, 1626; (d) H. Ziffer, K. Kabuto, D. T. Gibson, V. M. Kobal and D. M. Jerina, *Tetrahedron,* 1977, ***33,*** 2491; (e) G. J. Zylstra and D. T. Gibson, *J. Biol. Chem.,* 1989, **264**, 14940; (f) P. A. Williams and J. R. Sayers, *Biodegradation,* 1994, **5**, 195; (g) M. M. Abu-Omar, A. Loaiza and N. Hontzeas, *Chem. Rev*., 2005, **105**, 2227-2252.

3 S. Resnick, K. Lee and D. Gibson, *J. Ind. Microbiol. Biotechnol*., 1996, **17**, 438.

4 D. R. Boyd, N. D. Sharma, S. A. Haughey, M. A. Kennedy, B. T. McMurray, G. N. Sheldrake, C. C. R. Allen, H. Dalton and K. Sproule, *J. Chem. Soc. Perkin Trans. 1*, 1998, 1929.

5 D. S. Torok, S. M. Resnick, J. M. Brand, D. L. Cruden and D. T Gibson, *J. Bacteriol*., 1995, **177**, 5799.

6 M. A. Vila, V. Steck, S. Rodriguez Giordano, I. Carrera and R. Fasan, *ChemBioChem*, 2020, **21**, 1981.

7 J. Froese, M.-A. Endoma-Arias and T. Hudlicky, *Org. Process Res. Dev*., 2014, **18**, 801.

8 G. N. Sheldrake, in *Chirality in Industry: the commercial manufacture and application of optically active compounds* (Ed. A. N. Collins, G. N. Sheldrake and J. Crosby) John Wiley & Sons Ltd, Chichester, 1992, pp. 127.

9 (a) B. D. Erickson and F. Mondello, *J. Appl. Environ. Microbiol*., 1993, **59**, 3858; (b) N. Kimura, A. Nishi, M. Goto and K. Furukawa, *J. Bacteriol*., 1997, **179**, 3936; (c) T. Kumamaru, H. Suenaga, M. Mitsuoka, T. Watanabe and K. Furukawa, *Nat. Biotechnol*., 1998, **16**, 663; (d) S. Beil, J. R. Mason, K. N. Timmis and D. H. Pieper, *J. Bacteriol*., 1998, **180**, 5520; (e) N. Zhang, B. G. Stewart, J. C. Moore, R. L. Greasham, D. K. Robinson, B. C. Buckland and C. Lee, *Metab. Eng*., 2000, **2**, 339; (f) R. E. Parales, S. M. Resnick, C. L. Yu, D. R. Boyd, N. D. Sharma and D. T. Gibson, *J. Bacteriol*., 2000, **182**, 5495; (g) C. L. Yu, R. E. Parales and D. T. Gibson, *J. Ind. Microbiol. Biotechnol*., 2001, **27**, 94; (h) T. Sakamoto, J. M. Joern, A. Arisawa and F. H. Arnold, *Appl. Environ. Microbiol*., 2001, **67**, 3882; (i) J. M. Joern, T. Sakamoto, A. Arisawa and F. H. Arnold, *J. Biomol. Screening*, 2001, **6**, 219; (j) H. Suenaga, T. Watanabe, M. Sato, Ngadiman and K. Furukawa, *J. Bacteriol*., 2002, **184**, 3682; (k) R. E. Parales, *J. Ind. Microbiol. Biotechnol*., 2003, **30**, 271; (l) K. Pollmann, V. Wray, H. J. Hecht and D. H. Pieper, *Microbiology,* 2003, **149**, 903; (m) L. M. Newman, H. Garcia, T. Hudlicky and S. A. Selifonov, *Tetrahedron*, 2004, **60**, 729; (n) B. G. Keenan, T. Leungsakul, B. F. Smets, M. Mori, D. E. Henderson and T. K. Wood, *J. Bacteriol*., 2005, **187**, 3302; (o) E. L. Ang, J. P. Obbard and H. M. Zhao, *Appl. Microbiol. Biotechnol*., 2009, **81**, 1063; (p) P. Kumar, M. Mohammadi, J. F. Viger, D. Barriault, L. Gomez-Gil, L. D. Eltis, J. T. Bolin and M. Sylvestre, *J. Mol. Biol*., 2011, **405**, 531; (q) J. Seo, J.-Y. Ryu, J. Han, J.-H. Ahn, M. J. Sadowsky, H.-G. Hur and Y. Chong, *Appl. Microbiol. Biotechnol*., 2013, **97**, 693; (r) J. Shainsky, K. Bernath-Levin, S. Isaschar-Ovdat, F. Glaser and A. Fishman, *Protein Eng. Des. Sel*., 2013, **26**, 335; (s) D. Kim, M. Yoo, K. Y. Choi, B. S. Kang and E. Kim, *Bioresour. Technol*., 2013, **145**, 123; (t) K. Bernath-Levin, J. Shainsky, L. Sigawi and A. Fishman, *Appl. Microbiol. Biotechnol*., 2014, **98**, 4975; (u) C. Gally, B. M.

Nestl and B. Hauer, *Angew. Chem., Int. Ed*., 2015, **54**, 12952; (v) M. A. Vila, D. Umpierrez, N. Veiga, G. Seoane, I. Carrera and S. R. Giordano, *Adv. Synth. Catal*., 2017, **359**, 2149; (w) J. M. Halder, B. M. Nestl and B. Hauer, *ChemCatChem,* 2018, **10**, 178; (x) J. L. Wissner, J. T. Schelle, W. Escobedo-Hinojosa, A. Vogel and B. Hauer, *Adv. Synth. Catal*., 2021, **363**, 4905; (y) J. L. Wissner, W, Escobedo-Hinojosa, A. Vogel and B. Hauer, *J. Biotechnol*., 2021, **326**, 37; (z) P. M. Heinemann, D. Armbruster and B. Hauer, *Nat. Commun*., 2021, **12**, 1095; (aa) Y. Wang, C. Sun, J. Min, B. Li, J. Li, W. Chen, Y. Kong and X. Hu*, Int. Biodeter. Biodegr*., 2021, **161**, 105228.

10 E. A. Osifalujo, C. Preston-Herrera, P. C. Betts, L. R. Satterwhite and J. T. Froese, *ChemistrySelect*, 2022, **7**, e202200753.

11 R. E. Parales and S. M. Resnick, in *Biodegradation and Bioremediation. Soil Biology, Vol. 2* (Eds. A. Singh, O. P. Ward) Springer, Berlin, Heidelberg, 2007, pp. 175.

12 a) A. Karlsson, J. V. Parales, R. E. Parales, D. T. Gibson, H. Eklund and S. Ramaswamy, *Science* 2003, **299**, 1039; b) R. Friemann, K. Lee, E. N. Brown, D. T. Gibson, H. Eklund and S. Ramaswamy, *Acta Crys*. 2009, **D65**, 24.

13 C. Preston-Herrera, A. S. Jackson, B. O. Bachmann and J. T. Froese, *Org. Biomol. Chem*. 2021, **17**, 775.

14 T. D. Goddard, C. C. Huang, E. C. Meng, E. F. Pettersen, G. S. Couch, J. H. Morris and T. E. Ferrin, *Protein Sci*. 2018, **27**, 14.

15 a) L. Zheng, U. Baumann and J.-L. Reymond, *Nuc. Acids Res*. 2004, **32**, e115; b) H. Liu and J. H. Naismith, *BMC Biotechnology* 2008, **8**, 91.

16 J. Jumper, R. Evans, A. Pritzel, T. Green, M. Figurnov, O. Ronneberger, K. Tunyasuvunakool, R. Bates, A. Žídek, A. Potapenko, A. Bridgland, C. Meyer, S. A. A. Kohl, A. J. Ballard, A. Cowie, B. Romera-Paredes, S. Nikolov, R. Jain, J. Adler, T. Back, S. Petersen, D. Reiman, E. Clancy, M. Zielinski, M. Steinegger, M. Pacholska, T. Berghammer, S. Bodenstein, D. Silver, O. Vinyals, A. W. Senior, K. Kavukcuoglu, P. Kohli and D. Hassabis, *Nature* 2021, **596**, 583.

17 The PyMOL Molecular Graphics System, Version 2.0 Schrödinger, LLC.

18 O. Trott and A. J. Olson, *J. Comput. Chem*. 2010, **31**, 455.

19 a) D. van der Spoel, E. Lindahl, B. Hess, G. Groenhof, A. E. Mark and H. J. C. Berendsen, *J. Comp. Chem*. 2005, 26, 1701; b) S. Pronk, S. Páll, R. Schulz, P. Larsson, P. Bjelkmar, R. Apostolov, M. R. Shirts, J. C. Smith, P. M. Kasson, D. van der Spoel, B. Hess and E. Lindahl, *Bioinformatics*, 2013, **29**, 845; c) M. J. Abraham, T. Murtola, R. Schulz, S. Páll, J. C. Smith, B. Hess and E. Lindahl, *SoftwareX* 2015, **1**, 19.